

COHERENT TRANSITION RADIATION FROM TRANSVERSELY MODULATED ELECTRON BEAMS

A. Halavanau^{1,2}, D. Mihalcea¹, P. Piot^{1,2}, S. P. Antipov^{3,4}, J. G. Power³, W. Liu⁴,
 E. Wisniewski³, C. Whiteford³, N. Neveu^{3,5}, A. Benediktovitch^{6,7}, A. V. Tyukhtin⁸, S. N. Galyamin⁸

¹ Department of Physics and Northern Illinois Center for Accelerator & Detector Development, Northern Illinois University DeKalb, IL, USA

² Fermi National Accelerator Laboratory, Batavia, IL, USA

³ Argonne Wakefield Accelerator, Argonne National Laboratory, Lemont, IL, USA

⁴ Euclid Techlabs LLC, Bolingbrook, IL, USA

⁵ Illinois Institute of Technology, IL, USA

⁶ Belarusian State University, Department of Theoretical Physics and Astrophysics, Minsk, Belarus

⁷ Center for Free Electron Laser Science, DESY, Hamburg, Germany

⁸ Saint Petersburg State University, Saint Petersburg, Russia

Abstract

A transverse laser-shaping optical setup using microlens arrays (MLAs), previously developed and employed at Argonne Wakefield Accelerator (AWA), allows the formation of both highly uniform and modulated (patterned) beams. In the latter case, transverse modulation is imposed in the sub-millimeter scale. In the present study, we report the simulations of backward coherent transition radiation (CTR) emitted from a transversely modulated beam. We compare the case of a uniform round beam against different transverse modulation wavelengths by generating CTR on a steel target and measuring the autocorrelation function of the resulting radiation with an interferometer. We particularly focus on the differences between round and patterned beam distributions and discuss possible future applications of this setup in THz radiation generation.

INTRODUCTION

Microlens arrays (MLAs) are commonly known in laser technology as light condensers and are often used for transverse laser beam homogenization. An alternative application of the MLAs is the generation of patterned beams that can be used in photoinjectors for multiple purposes [1].

Microlens array consists of periodically placed lenses forming a rectangular, honeycomb, or circular pattern. The resulting modulated light distribution mimics the microlens array geometry. The modulated pattern generated at the photocathode can be preserved and propagated downstream of the accelerator, while the spacing between the beamlets is controlled via solenoid and quadrupole lenses. Such an experimental setup was recently established at Argonne Wakefield Accelerator (AWA) facility [1], see Fig. 1.

Coherent transition radiation (CTR) is commonly used in temporal profile diagnostics [2–8]. An experimental setup usually consists of a retractable metallic screen and radiation diagnostics operating in the THz regime. Such a setup is depicted in Fig. 1 (a) and was recently built at AWA facility.

The goal of this study is to utilize MLA setup to introduce transverse modulation in the electron beam and observe its effect on the resulting CTR spectrum.

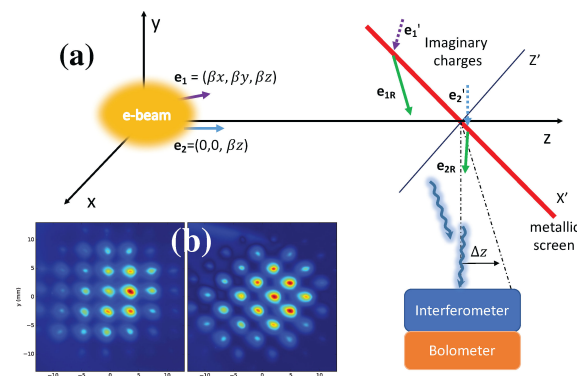


Figure 1: (a) Schematic of the experiment: an electron beam is incident on a metallic screen positioned at 45 deg. The resulting transition radiation photons are received in bolometer via interferometer transport to perform an auto-correlation scan. (b) An example of MLA-formed electron beam patterns observed at $\gamma = 100$.

SIMPLIFIED ANALYTICAL CALCULATION

A detailed analytical derivation of the transition radiation from a point charge as a solution of Maxwell's equations between two media can be found in classical textbooks [9, 10]. The electromagnetic field of a point charge falling onto a metallic plate can be calculated using the “method of images” [11], where for every charge incident on an infinite plane (q, \mathbf{e}_i) there is a “mirror” charge (q', \mathbf{e}'_i) behind the plane forming a pair of real and image charges. When a virtual pair of charges approaches the plane, it emits radiation that is mathematically equivalent to the transition radiation from a point charge [10]¹.

¹ Additionally, an analytical expression for a TR EM-field in case of a finite metallic plane can be found in [12].

Content from this work may be used under the terms of the CC BY 3.0 licence (© 2018). Any distribution of this work must maintain attribution to the author(s), title of the work, publisher, and DOI.

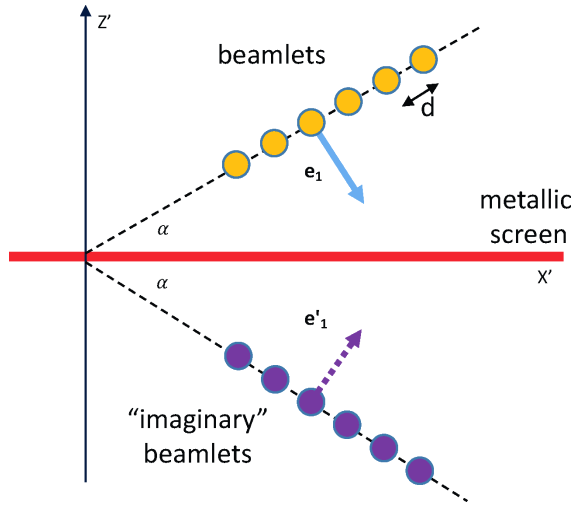


Figure 2: Simplified schematics of the “line” charge arrangement with spacing d . Axes correspond to Figure 1 notations.

Assume a “line” formation of point charges with spacing d arriving in parallel at the infinite metallic screen. Figure 2 illustrates such an arrangement for both “real” and “imaginary” charges.

A magnetic component of a TR EM-field can be written as [10]:

$$\vec{H}_\omega = \frac{q}{2\pi c} \sum_{i=1}^N \left(\frac{\vec{e}_{iR} \times \vec{e}_i}{1 - \vec{e}_{iR} \cdot \vec{e}_i} - \frac{\vec{e}'_{iR} \times \vec{e}'_i}{1 - \vec{e}'_{iR} \cdot \vec{e}'_i} \right) \times \frac{\exp(i\omega R_i/c + i\omega t_i)}{R_i}, \quad (1)$$

where N is the number of charges q , \vec{e}_i is the velocity vector, \vec{e}_{iR} is the vector from the point of incidence to the detector, R_i is the distance from the point of incidence to the detector, t_i is the time of arrival of i -th charge at the metallic plate, ω is the radiation frequency. The spectral density of the radiation can then be computed as [10]:

$$\frac{d^2W}{d\omega d\Omega} = cR^2 |\vec{H}_\omega|^2 \quad (2)$$

Assuming the detector is far from the plate, Eq. 1 can be rewritten as:

$$\vec{H}_\omega \approx \frac{q}{2\pi cR} \vec{f} \sum_{i=1}^N \exp(i\omega R_i/c + i\omega t_i), \quad (3)$$

where $\vec{f} = \left(\frac{\vec{e}_R \times \vec{e}}{1 - \vec{e}_R \cdot \vec{e}} - \frac{\vec{e}'_R \times \vec{e}'}{1 - \vec{e}'_R \cdot \vec{e}'} \right)$ and the term under summation can be referred as a bunching factor:

$$F = \left| \sum_{i=1}^N \exp(i\omega R_i/c + i\omega t_i) \right|^2 \quad (4)$$

Note, if the detector is located in the far-zone, the particles with the same t_i will have almost the same contribution to the resulting spectrum. Nevertheless, the path difference

ΔR_i is finite, therefore has to be accounted for. The resulting spectral density can be then rewritten in a shorter form:

$$\frac{d^2W}{d\omega d\Omega} \approx \frac{q^2}{4\pi^2 c} f^2 F \quad (5)$$

NUMERICAL SIMULATIONS

To perform numerical simulations, a code that computes radiation spectral density (Eq. (2)) with exact expression for \vec{H}_ω (Eq. (1)) and approximation (Eq. (3)) was developed. The results were found to be very close, therefore hereafter we will refer to the calculations via Eq. (3). $N = 8000$ particles were used in simulations of both transverse Gaussian bunches and beamlets arranged in a vertical “line” with a spacing of $d = 1$ mm. The longitudinal bunch length was assumed to be Gaussian with $\sigma_z \ll d$. The detector was assumed to be in a far-zone meaning $R \gg 8$ mm. In the simulations, the electron beam was assumed to have a waist at the location of the metallic screen and transverse emittance was set to 0.

TR is known to have a “double-horn” structure, which is independent of transverse electron distribution and attributed to the fact that there is no radiation emitted along the direction perpendicular to the charge velocity [9, 10]. Such a spectrum is displayed in Fig. 3 for the case of a Gaussian and modulated transverse distribution. The simulation was done for the same number of particles in both cases and the 3σ size of the Gaussian distribution was matched by the beamlet array size.

The spectral content of the radiation generated by a Gaussian bunch and 8 beamlets arranged in a “line” is depicted in Fig. 4. The beamlet pattern possesses a peculiar spectral structure in the THz regime. As it can be seen in Fig. 4, additional radiation peaks emerge at detector offsets of about 2° , while the maximum of the radiation is contained around 0.57° . The first harmonic seems to be relatively narrow-band, therefore motivating the experimental attempt.

The numerical study with realistic beam distributions will be performed in the near future and reported elsewhere.

EXPERIMENTAL SETUP

A numerical model of the AWA-DB beamline was established in OPAL-T, IMPACT-T, GPT and ASTRA [13–16]. Electron beam simulations were performed to achieve necessary beam parameters at the location of the metallic screen [17, 18].

In the experimental setup we use two MLA plates of a rectangular spacing with $300 \mu\text{m}$ pitch and $f = 5$ mm focal length. The MLAs are illuminated with mJ-energy 248 nm laser pulses. Such a configuration provides very flexible spatial shaping technique, therefore it is routinely employed in various AWA electron beam experiments [1]. The electrons are accelerated to 7 MeV in an L-band RF gun and further transported through 6 L-band linacs to a final energy of up to 72 MeV; see [19].

A stainless steel mirror is installed in the beamline at $\alpha = 45^\circ$ after the last accelerating structure with an interferometer and bolometer on the side; see Fig 1. For a detailed

Content from this work may be used under the terms of the CC BY 3.0 licence (© 2018). Any distribution of this work must maintain attribution to the author(s), title of the work, publisher, and DOI.

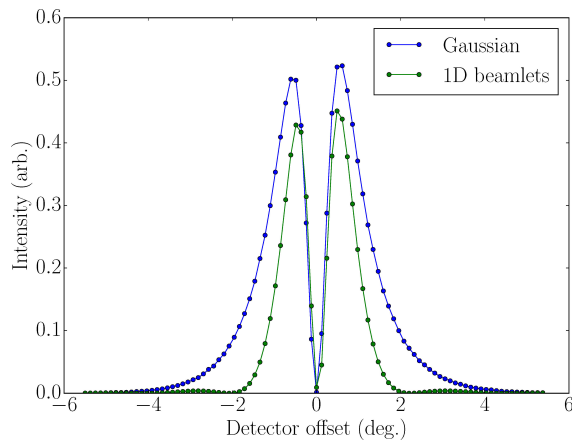


Figure 3: Simulated “double-horn” TR spectrum calculated at $\omega = 6$ THz for the detector configuration shown in Fig. 1. Beamlet “line” arrangement consisted of 8 beamlets with spacing $d = 1$ mm.

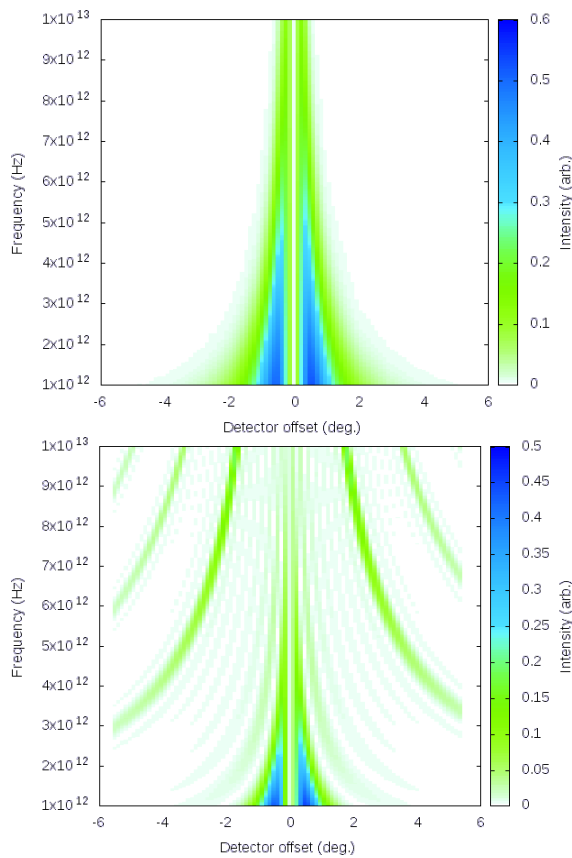


Figure 4: Spectral content of the Gaussian (top) and 8 beamlets “line” arrangement (bottom) with spacing of $d = 1$ mm.

description of the interferometer please see [8]. A IR-Labs general purpose LN-6/C 4.2 K bolometer [20] is installed downstream of the interferometer.

Such a setup allows autocorrelation scans of the electron beam, revealing it’s spectral content. Additionally, the MLAs were placed on a rotatable stage to compensate the Larmor rotation in the RF gun solenoids and allow for different pattern angles at the CTR mirror; see Fig 1 (b).

EXPERIMENTAL PLAN

The experiment will be performed as follows. A transversely homogenized laser distribution will be created in the MLA setup and transferred onto photocathode. The beamline will be tuned to provide the beam waist at the location of the metallic screen. An interferometer will be used for an autocorrelation scan with the CTR signal registered in bolometer. This data will be used for the bunch length measurement. The MLA setup will then be switched to the beamlet mode and the electron beamlet distribution will be propagated onto the screen. The same measuring technique will be used to compare the spectral contents between the two cases. A mechanical scanning slit will be used to introduce detector offset, allowing for measurement of the narrow-band part of the spectrum. The beamlet spacing will be determined by the bunch length, and imposed by using quadrupole magnets upstream of the screen.

CONCLUSIONS

We demonstrated via numerical simulations the possibility of generating THz coherent transition radiation via electron beam transverse shaping. The resulting spectral content is different from the Gaussian transverse distribution, with narrow-band harmonics present in the THz range. The limiting factor is found to be the bunch length which has to be significantly shorter than beamlet spacing. The particle distribution along the vertical axis has a leading effect in generating transverse CTR, while the distribution along the horizontal axis is a second-order effect. A preliminary experiment confirmed the difference in CTR spectrum due to transverse beam modulation. A follow-up experiment is scheduled at AWA facility and the results will be reported shortly.

REFERENCES

- [1] A. Halavanau, G. Qiang, G. Ha, E. Wisniewski, P. Piot, J. G. Power, and W. Gai, "Spatial Control of Photoemitted Electron Beams using a Micro-Lens-Array Transverse-Shaping Technique", arxiv:1707.08448, submitted to PRAB, (2017).
- [2] U. Happek, A. J. Sievers, and E. B. Blum, "Observation of coherent transition radiation", *Phys. Rev. Lett.*, 67:2962–2965, (1991).
- [3] W. Barry, "Measurement of subpicosecond bunch profiles using coherent transition radiation", *AIP Conference Proceedings*, 390(1):173–185, (1997).
- [4] Y. Shibata, T. Takahashi, T. Kanai, K. Ishi, M. Ikezawa, J. Ohkuma, S. Okuda, and T. Okada, "Diagnostics of an electron beam of a linear accelerator using coherent transition radiation", *Phys. Rev. E*, 50:1479–1484, (1994).
- [5] C. Settakorn, "Generation and use of coherent transition radiation from short electron bunches", PhD thesis, Stanford University (2001).
- [6] T. J. Maxwell, "Measurement of Sub-Picosecond Electron Bunches via Electro-Optic Sampling of Coherent Transition Radiation", PhD thesis, Northern Illinois U. (2012).

- [7] S. Antipov, C. Jing, M. Fedurin, W. Gai, A. Kanareykin, K. Kusche, P. Schoessow, V. Yakimenko, and A. Zholents, "Experimental observation of energy modulation in electron beams passing through terahertz dielectric wakefield structures", *Physical review letters*, 108(14):144801, (2012).
- [8] D. Mihalcea, C. L. Bohn, U. Happek, and P. Piot, "Longitudinal electron bunch diagnostics using coherent transition radiation", *Phys. Rev. ST Accel. Beams*, 9:082801, (2006).
- [9] D. J. Jackson, *Classical Electrodynamics*. Wiley, 1998. New York.
- [10] V. L. Ginzburg and V. N. Tsytovich, *Transition Radiation and Transition Scattering*. Hilger, 1990. London.
- [11] V. N. Krasilnikov and A. V. Tyukhtin, "Reflection theorems for some anisotropic media", *Radiophysics and Quantum Electronics*, 27, 717-723 (1984).
- [12] S. Casalbuoni, B. Schmidt, P. Schmüser, V. Arsov, and S. Wesch, "Ultrabroadband terahertz source and beamline based on coherent transition radiation", *Phys. Rev. ST Accel. Beams*, 12:030705 (2009).
- [13] A. Adelman, A. Gsell, V. Rizzoglio, C. Metzger-Kraus, Y. Ineichen, X. Pang, S. Russell, C. Wang, J. Yang, S. Sheehy, C. Rogers, and D. Winklehner, "The opal framework", PSI-PR-08-02.
- [14] J. Qiang, *IMPACT-T reference manual*, LBNL-62326, (2007).
- [15] S.B. van der Geer *et al.*, "3d space-charge model for gpt simulations of high brightness electron bunches", *Institute of Physics Conference Series*, 175:101, (2005).
- [16] K. Flöttmann, *ASTRA reference manual*, DESY (2000).
- [17] N. Neveu, J. Larson, J. G. Power, and L. Spentzouris, "Photoinjector optimization using a derivative-free, model-based trust-region algorithm for the argonne wakefield accelerator", *Journal of Physics: Conference Series*, 874(1):012062, (2017).
- [18] N. Neveu *et al.*, "Benchmark of RF Photoinjector and Dipole Using ASTRA, GPT, and OPAL", in *Proc. of NAPAC'16*, Chicago, USA, paper THPOA46, (2016).
- [19] M.E. Conde *et al.*, in *Proceedings of IPAC'10*, Kyoto, Japan, paper THPD016, (2010).
- [20] IR Labs, <http://www.infraredlaboratories.com/home.html>